Malaysian Journal of Analytical Sciences (MJAS)



Published by Malaysian Analytical Sciences Society

FACILE CHEMICAL SYNTHESIS OF PURE Zn DOPED CeO₂ NANOPARTICLES WITH ENHANCED PHOTOCATALYTIC PERFORMANCE UNDER UV IRRADIATION

(Sintesis Kimia Mudah bagi Nanopartikel CeO₂ Dop Zn Tulen dengan Prestasi Fotokatalitik yang Dipertingkatkan di bawah Penyinaran UV)

Swathi Chidaraboyina^{1,3}, Arputharaj Samson Nesaraj¹,^{2*}, Manasai Arunkumar¹

¹Department of Applied Chemistry,
Karunya Institute of Technology and Sciences (Deemed to be University),
Karunya Nagar, Coimbatore – 641 114, Tamil Nadu, India

²Department of Chemistry,
Kalasalingam Academy of Research and Education (Deemed to be University), Anand Nagar,
Krishnankoil – 626 126, Tamil Nadu, India

³Department of Chemistry, Keshav Memorial Institute of Technology, 3-5-1026, Narayanaguda,
Hyderabad – 500 029, Telengana, India

*Corresponding author: samson@klu.ac.in

Received: 5 August 2022; Accepted: 10 November 2022; Published: 22 February 2023

Abstract

Rhodamine B (RhB) is an organic dye which is generally used in paint, paper and textile industries as a tracer dye. It is found to be highly toxic to living organisms and is expected of having carcinogenic effect. Therefore, the effluents containing RhB dye should be properly treated before releasing into water bodies, such as, rivers, ponds, etc. In this research work, attempts were made to prepare and use zinc doped ceria ($Ce_{1-x}Zn_xO_{2-\delta}$; x=0,0.1,0.2,0.3,0.4,0.5) nanoparticles as photocatalysts to remove RhB dye present in water. These nanoparticles were synthesized by simple wet chemical technique using cheap chemicals. The prepared materials were analyzed by X-ray diffraction (XRD), Fourier transform infra-red (FTIR), Energy-dispersive X-ray spectroscopy (EDX), scanning electron microscope (SEM), ultra violet-visible (UV-Vis) and photo-luminescence (PL) spectroscopy methods. The samples were indexed in face-centered cubic (FCC) crystalline structure. FTIR showed M-O bond in the samples. EDX notified the occurrence of appropriate elements. SEM exhibited smaller and bigger grains in the materials. The λ_{max} was found to be 349 nm by UV-visible analysis. The band gap energy (Eg) was reported in the range of 1.5-3 eV. The photoluminescence spectra for all suspensions were obtained in the range of 390 to 550nm. Then, the photocatalytic elimination of Rhodamine B (Rh B) with the help of $Ce_{1-x}Zn_xO_{2-\delta}$ nano-photocatalysts under UV light was studied. Among the several trials studied, highest photodegradation efficiency (58.71%) was found at pH=11 after 60 minutes irradiation in UV light at room temperature for $Ce_{0.60}Zn_{0.40}O_{2-\delta}$.

Keywords: Zn doped CeO2 nanoparticles, Rhodamine B, dye removal, photocatalytic degradation, UV irradiation

Abstrak

Rhodamine B (RhB) ialah pewarna organik yang biasanya digunakan dalam industri cat, kertas dan tekstil sebagai pewarna pengesan. Ia didapati sangat toksik kepada organisma hidup dan dijangka mempunyai kesan karsinogenik. Oleh itu, efluen yang

mengandungi pewarna RhB hendaklah dirawat dengan betul sebelum dilepaskan ke dalam badan air, seperti sungai, kolam, dsb. Dalam kerja penyelidikan ini, percubaan telah dibuat untuk menyediakan dan menggunakan ceria terdop zink (Ce_{1-x}Zn_xO_{2-δ}; x = 0, 0.1, 0.2, 0.3, 0.4, 0.5) nanopartikel sebagai fotomangkin untuk menghilangkan pewarna RhB yang terdapat dalam air. Nanopartikel ini telah disintesis dengan teknik kimia basah mudah menggunakan bahan kimia murah. Bahan-bahan yang disediakan telah dianalisis dengan pembelauan sinar-X (XRD), infra merah transformasi Fourier (FTIR), spektroskopi sinar-X penyebaran tenaga (EDX), mikroskop elektron pengimbasan (SEM), Ultra ungu-cahaya nampak (UV-Vis) dan kaedah spektroskopi foto-pendarcahaya (PL). Sampel telah diindeks dalam struktur hablur kubik berpusat muka (FCC). FTIR menunjukkan ikatan M-O dalam sampel. EDX memberitahu berlakunya elemen yang sesuai. SEM mempamerkan butiran yang lebih kecil dan lebih besar dalam bahan. λ_{maks} didapati 349 nm oleh analisis UV-cahaya nampak. Tenaga jurang jalur (Eg) dilaporkan dalam julat 1.5-3 eV. Spektrum foto-pendarcahaya untuk semua suspensi diperoleh dalam julat 390 hingga 550nm. Kemudian, penghapusan fotomangkin Rhodamine B (Rh B) dengan bantuan fotomangkin nano Ce_{1-x}Zn_xO_{2-δ} di bawah cahaya UV telah dikaji. Antara beberapa ujian yang dikaji, kecekapan fotodegradasi tertinggi (58.71%) didapati pada pH=11 selepas 60 minit penyinaran dalam cahaya UV pada suhu bilik untuk Ce_{0.60}Zn_{0.40}O_{2-δ}.

Kata kunci: nanopartikel CeO2 terdop Zn, Rhodamine B, penyingkiran pewarna, degradasi fotokatalitik, penyinaran UV

Introduction

Prestigious revolution by nanoscience especially nano metal oxides is being noticed nowadays because of its tremendous application in the fabrication of medical devices [1-4], sensors [5-7], photo catalysts [8-10], etc. The pollutants in particular organic dyes released by the textile industries are affecting the environment seriously. Hence, the elimination of organic dye molecules from the effluent water of textile industry is an urgent issue. Among different organic dyes reported, Rhodamine B is found to be highly harmful when swallowed, with acute oral toxicity, causes serious eye damage or irritation, hazardous to the aquatic environment with long-term side effects [11]. Different technologies, such as, adsorption, ozonation, advanced oxidation process (AOP), membrane filtration, biological methods [12-13] have been tried across the globe for the past two decades to remove the variety of organic dyes present in water. AOP was found to be good in removing different kind of dye molecules and other organic effluents [14-16].

Recently, it was noticed that photocatalysis can also be involved in degrading the organic dyes present in the textile effluents [17]. Metal oxide nanoparticles were found to be effective as photocatalysts [18]. Ceric oxide (CeO₂) is a widely used rare earth oxide material with attractive scientific, technological, energy and environmental applications [19]. The physico-chemical properties, such as, photoluminescence and photocatalytic activity were improved by doping Zn in Ce site of CeO₂ [20]. Further, 1% nickel (Ni) doping was

found to retard the band gap of undoped ceria, which could be associated with the reduction of the average crysllite size and therefore, it is considered to be an optimum dopant for ceria [21]. The thermal stability of CeO₂ was improved by doping lanthanum (La) [22]. Iron (Fe) doped CeO₂ nanoparticles exhibited excellent dielectric properties and antimicrobial activity especially in the persistence of bacterial infection [23].

In this research work, to improve the material characteristics of ceria, the metal ion like Zn is doped in cerium lattice of CeO_2 with varying concentration. It was reported that doping Zn into CeO_2 could result in better UV absorptivity [24]. The present study deals with two parts. The first part involves the synthesis and characterization of zinc doped ceria ($Ce_{1-x}Zn_xO_{2-\delta}$; x=0,0.1,0.2,0.3,0.4,0.5) nanoparticles. The second part is about the photocatalytic studies of zinc doped ceria nanomaterials in degrading the Rh B dye found in the water sample under UV light illumination. The obtained experimental results were analyzed in a detailed manner in this research article.

Materials and methods

Chemicals and reagents

Analytical grade of ceric nitrate hexahydrate, zinc nitrate hexahydrate, sodium hydroxide and ethanol were procured and used in this study as such.

Material preparation

Stoichiometric quantities of metal nitrates (cerous nitrate and zinc nitrate) were dissolved in ultra-pure

water. The precipitant solution (NaOH) was mixed drop-wise to the metal nitrate salts solution with constant stirring in a magnetic stirrer. The pH of the solution was kept above pH 9 during the course of the reaction. The resultant precipitate (cerium hydroxide and zinc hydroxide mixture) was filtered-off using Whatman filter paper and cleaned thoroughly without any impurities using the mixture of distilled water and

ethanol (9:1 v/v). Then, the precipitate mixture was dried in an air oven and calcined at 600 °C. This resulted as a pure $Ce_{1-x}Zn_xO_{2-\delta}$ (where $x=0,\,0.1,\,0.2,\,0.3,\,0.4$ and 0.5) nanoparticles. The amount of chemicals used to prepare the materials is indicated in Table 1. The possible reaction mechanism for this preparation is indicated in Equation 1.

$$(1-x) Ce(NO_3)_3 + x Zn(NO_3)_2 + 2 NaOH \rightarrow Ce_{1-x}Zn_xO_{2-\delta} + 2 NaNO_3 + y H_2O$$
 (eq. 1)

where x = 0, 0.1, 0.2, 0.3, 0.4 and 0.5

Characterization of materials

X-ray diffraction measurement (XRD) was conducted using X-ray diffractometer (in Shimadzu XRD 6000) at 30 mA current and voltage of 40kV involved the usage of Cuk_{α} (K=0.154059nm) radiation with a nickel filter. The 2θ scanning range was 2° to 80° at a continuous scan mode with a scan speed of 10° /min. The unit cell parameter was measured by DOS computer programming. The average crystallite size for the samples was determined by Debye –Scherrer's formula. Fourier-Transform infrared (FT-IR) spectra of parent CeO₂ and Zn doped CeO₂ nanoparticles was measured by Shimadzu (IR Prestige 21) FTIR spectrophotometer,

using KBr pellet technique in the range of 4000 to 400 cm⁻¹. Scanning electron microscopy (SEM) was performed to detect the surface morphology and the elemental composition of parent CeO₂ and Zn doped CeO₂ nanoparticles (SEM JEOL JSM-6610) equipped with an energy dispersive X-ray (EDAX) spectrophotometer which is operated at 20kV. The band gap of synthesized pure CeO₂ and Zn doped CeO₂ nanoparticles was determined by UV spectrophotometer (Shimadzu 1800). The synthesized samples were loaded into a quartz experimental set-up and the spectrum was recorded using absorbance method.

Table 1. Amount of precursor salts used for the synthesis of CeO₂ and Zn doped CeO₂ nanoparticles [Volume of each solution is 10 mL]

Sample	Weight of Ce(NO ₃) ₃	Weight of Zn(NO ₃) ₂	Weight of NaOH
	(g)	(g)	(g)
CeO ₂	4.342	=	1.6
$Ce_{0.90}Zn_{0.10}O_{2\text{-}\delta}$	3.907	0.297	1.6
$Ce_{0.80}Zn_{0.20}O_{2\text{-}\delta}$	3.473	0.594	1.6
$Ce_{0.70}Zn_{0.30}O_{2\text{-}\delta}$	3.039	0.892	1.6
$Ce_{0.60}Zn_{0.40}O_{2\text{-}\delta}$	2.605	1.189	1.6
$Ce_{0.50}Zn_{0.50}O_{2-\delta}$	2.171	1.487	1.6

Photocatalytic experiment

To understand the photocatalytic behavior of Zn doped CeO₂ nanoparticles, Rhodamine B dye was used. For each experiment, 50 mL of RhB dye solution (0.005g of RhB dye was dissolved in one liter of ultra-pure water to make a solution) was mixed with 0.02g of Zn doped CeO₂ nanoparticles and kept in dark for 30 minutes until

reach equilibrium. The sample was irradiated to the UV light and the study was carried out at 0, 15, 30, 45 and 60 minutes intervals and centrifuged. 3 mL of the photo reacted solutions was taken for UV-visible spectroscopy measurements at a wavelength of 554 nm. The removal efficiency and percentage of degradation of dye was determined using the Equation 2.

Percentage of degradation of dye = $(C_0-C_t/C_0)*100$

(eq. 2)

where, 'C_o' is the initial absorbance of the dye solution (Rh B solution) and 'C_t' is the absorbance of RhB dye solution after the photodegradation reaction, i.e., after certain time 't'.

Results and Discussion

XRD studies

The crystalline behavior of the prepared materials was analyzed by XRD. The XRD patterns obtained on Zn doped CeO₂ nanoparticles are reported in Figure 1. The resultant XRD results were matched well with the standard CeO₂ data (JCPDS No. 65-5923). diffraction peaks found at 2θ values of 28.62° , 33.17°, 47.59°, 56.45°, 59.20° and 69.51° corresponding to (111), (200), (220), (311), (222) and (400) crystal planes respectively whose hkl values were concurrent with the reported data [25-27]. No impurity peaks relevant to any impurity phases were seen in the XRD diagrams. The crystalline structure of all compositions of CeO2 was found to be face centered cubic (FCC). The crystallite size, Dx, was calculated by using Debye-Scherrer formula (Equation 3):

$$D_{x} = K\lambda/\beta \cos\theta \qquad (eq. 3)$$

where, β is the full width at half maximum (FWHM) of a diffraction peak, K is the shape factor approx. 0.91, λ is the wavelength of the X-ray source that equals 1.54 Å and θ is the Bragg's angle. The calculated crystallite size values of Zn doped CeO₂ are presented in Table - 2. The crystallite size of the samples varied between ranges from 20.47 to 22.04 nm. The theoretical density (D_p) was calculated by using the formula (Equation 4),

$$D_p = Z*M/NxV (g.cm^{-3})$$
 (eq. 4)

where, Z is the number of chemical species in the unit cell, M is the molecular mass of the sample (g/mol), N is the Avogadro's number (6.023 x 10 ²³) and V is the unit cell volume equals to a³ which is the lattice constant in cm. From the XRD data, it was found that there is no much variation in the unit cell parameter and unit cell volume of Zn doped CeO₂ samples. The XRD parameters were compared with the Joint Committee on Powder Diffraction Standards (JCPDS) data. Theoretical density values got reduced with regard to the enhancement of dopant concentration as reported in the literature [28].

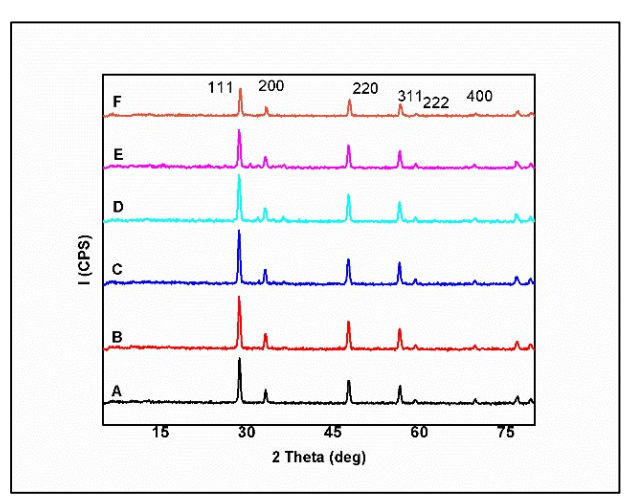


Figure 1. XRD patterns obtained on CeO_2 based nanoparticles a) Pure CeO_2 , b) $Ce_{0.90}Zn_{0.10}O_{2-\delta}$, c) $Ce_{0.80}Zn_{0.20}O_{2-\delta}$, d) $Ce_{0.70}Zn_{0.30}O_{2-\delta}$, e) $Ce_{0.60}Zn_{0.40}O_{2-\delta}$, and f) $Ce_{0.50}Zn_{0.50}O_{2-\delta}$

, , ,	1	-		- 1	2
Sample	Crystal Structure	Unit Cell Parameter (Å)	Unit Cell Volume (ų)	Crystallite Size (nm)	Theoretical Density (gcm ⁻³)
CeO ₂	Cubic (F.C)	5.39	156.59	20.69	7.30
$Ce_{0.90}Zn_{0.10}O_{2-\delta}$	Cubic (F.C)	5.40	157.46	22.13	6.92
$Ce_{0.80}Zn_{0.20}O_{2-\delta}$	Cubic (F.C)	5.40	157.46	20.58	6.60
$Ce_{0.70}Zn_{0.30}O_{2\text{-}\delta}$	Cubic (F.C)	5.40	157.46	22.04	6.28
$Ce_{0.60}Zn_{0.40}O_{2\text{-}\delta}$	Cubic (F.C)	5.40	157.46	20.47	5.96
$Ce_{0.50}Zn_{0.50}O_{2-\delta}$	Cubic (F.C)	5.40	157.46	20.90	5.65

Table 2. Crystallographic parameters obtained on CeO₂ and Zn doped CeO₂ nanoparticles by XRD analysis

FTIR studies

The FTIR analysis for all the samples were measured at room temperature. FTIR spectra obtained on Zn doped CeO₂ nanoparticles are shown in Figure 2. The absorption bands observed in the range of 600 cm⁻¹ attribute to the stretching vibration modes of M-O [29]. FTIR showed a weak band at 842 cm⁻¹ which may be

due to the presence of CO₃²⁻ in the sample. Peak appeared at 1384 cm⁻¹ may be due to the presence of NO₃⁻ in the sample. Peak appeared at 1700 cm⁻¹ may be due to the presence of carboxylic acid in the sample. The above peaks were reported in the final product because of trace level of organic and inorganic impurities present in the sample as reported [30].

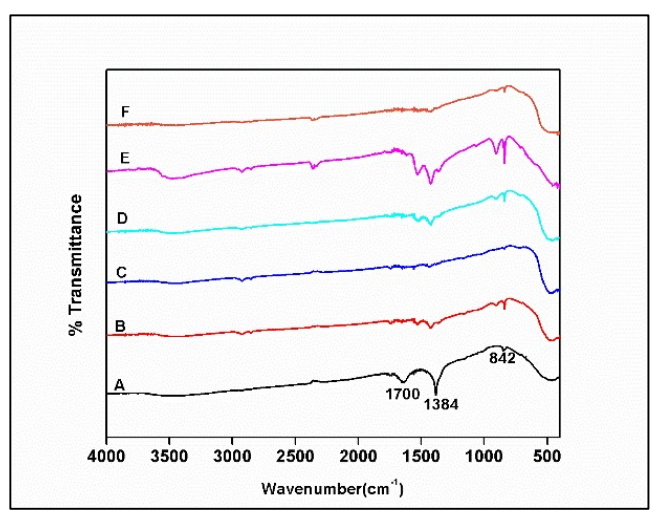


Figure 2. FTIR spectra obtained on CeO_2 based nanoparticles a) Pure CeO_2 , b) $Ce_{0.90}Zn_{0.10}O_{2-\delta}$, c) $Ce_{0.80}Zn_{0.20}O_{2-\delta}$, d) $Ce_{0.70}Zn_{0.30}O_{2-\delta}$, e) $Ce_{0.60}Zn_{0.40}O_{2-\delta}$, f) $Ce_{0.50}Zn_{0.50}O_{2-\delta}$

Elemental analysis

The EDX spectra obtained on Zn doped CeO₂ based nanoparticles are shown in Figure 3 and the corresponding data are presented in Table 3. From the data, it was confirmed that appropriate quantities of Ce,

Zn and O alone are present in the samples. No impurity elements were seen. So, all the synthesized materials are pure. The product formed is well matched with stoichiometric weight of the corresponding elements.

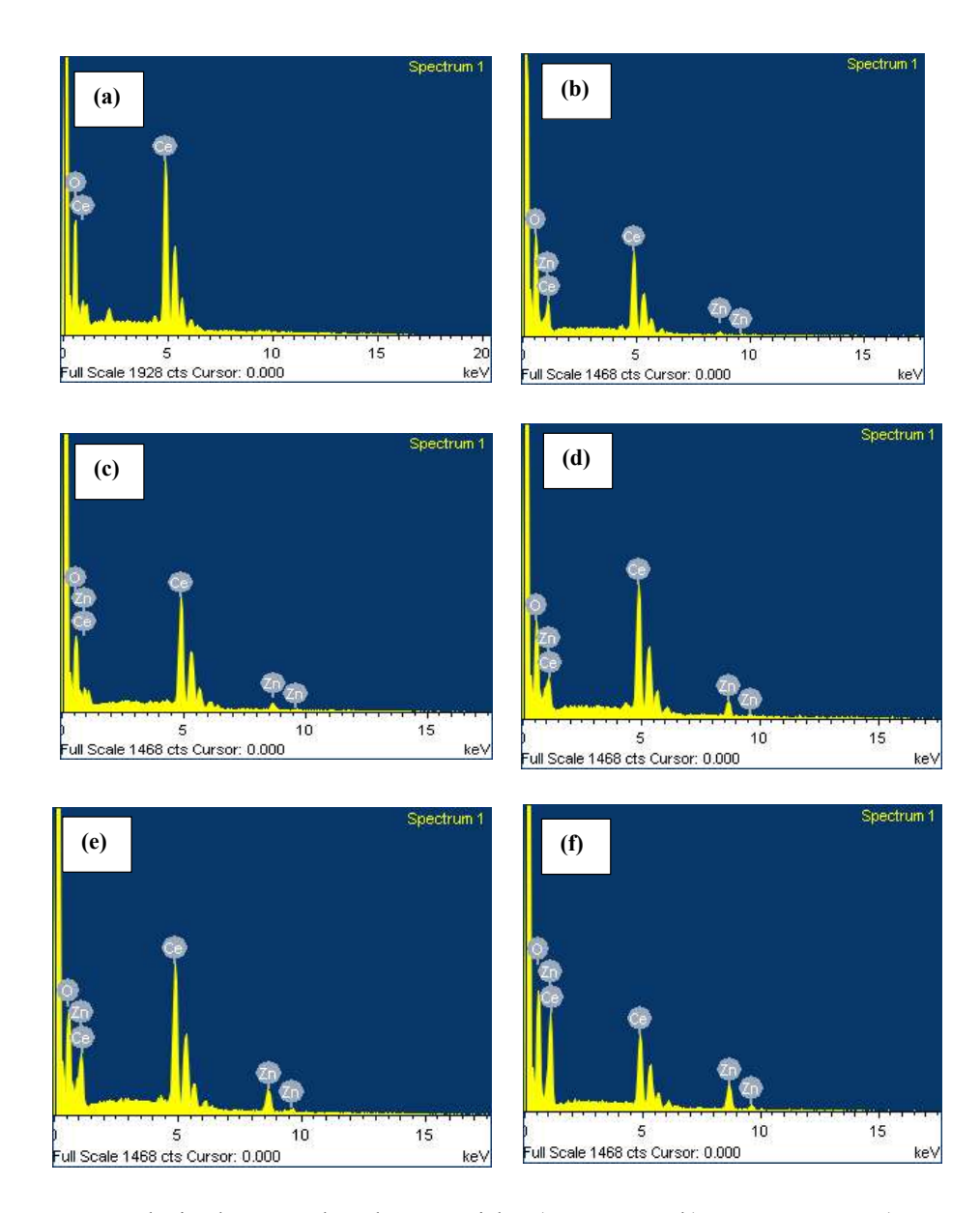


Figure 3. EDAX patterns obtained on CeO₂ based nanoparticles a) Pure CeO₂, b) $Ce_{0.90}Zn_{0.10}O_{2-\delta}$, c) $Ce_{0.80}Zn_{0.20}O_{2-\delta}$ δ , d) $Ce_{0.70}Zn_{0.30}O_{2-\delta}$, e) $Ce_{0.60}Zn_{0.40}O_{2-\delta}$ and f) $Ce_{0.50}Zn_{0.50}O_{2-\delta}$

Morphological study

The SEM photographs of Zn doped CeO₂ nanoparticles are presented in Figure 4. The grain size was found to be 200 to 300 nm. The presence of bigger sized grains in the sample may be due to the agglomeration effect

because of high temperature calcination process. Suitable heating rate needs to be followed during calcination which can control the grain growth of the materials [31].

Sample	Cerium		Zinc		Oxygen	
	Atomic %	Weight %	Atomic %	Weight %	Atomic %	Weight %
CeO ₂	26.23	75.7	-	-	73.77	24.30
$Ce_{0.90}Zn_{0.10}O_{2\text{-}\delta}$	16.92	62.59	1.78	3.08	81.30	34.33
$Ce_{0.80}Zn_{0.20}O_{2\text{-}\delta}$	24.00	70.23	4.25	5.80	71.76	23.98
$Ce_{0.70}Zn_{0.30}O_{2\text{-}\delta}$	22.05	65.68	7.45	10.35	70.5	23.97
$Ce_{0.60}Zn_{0.40}O_{2\text{-}\delta}$	21.61	63.72	9.53	13.10	68.86	23.18
$Ce_{0.50}Zn_{0.50}O_{2\text{-}\delta}$	11.51	44.96	11.32	20.63	77.17	34.42

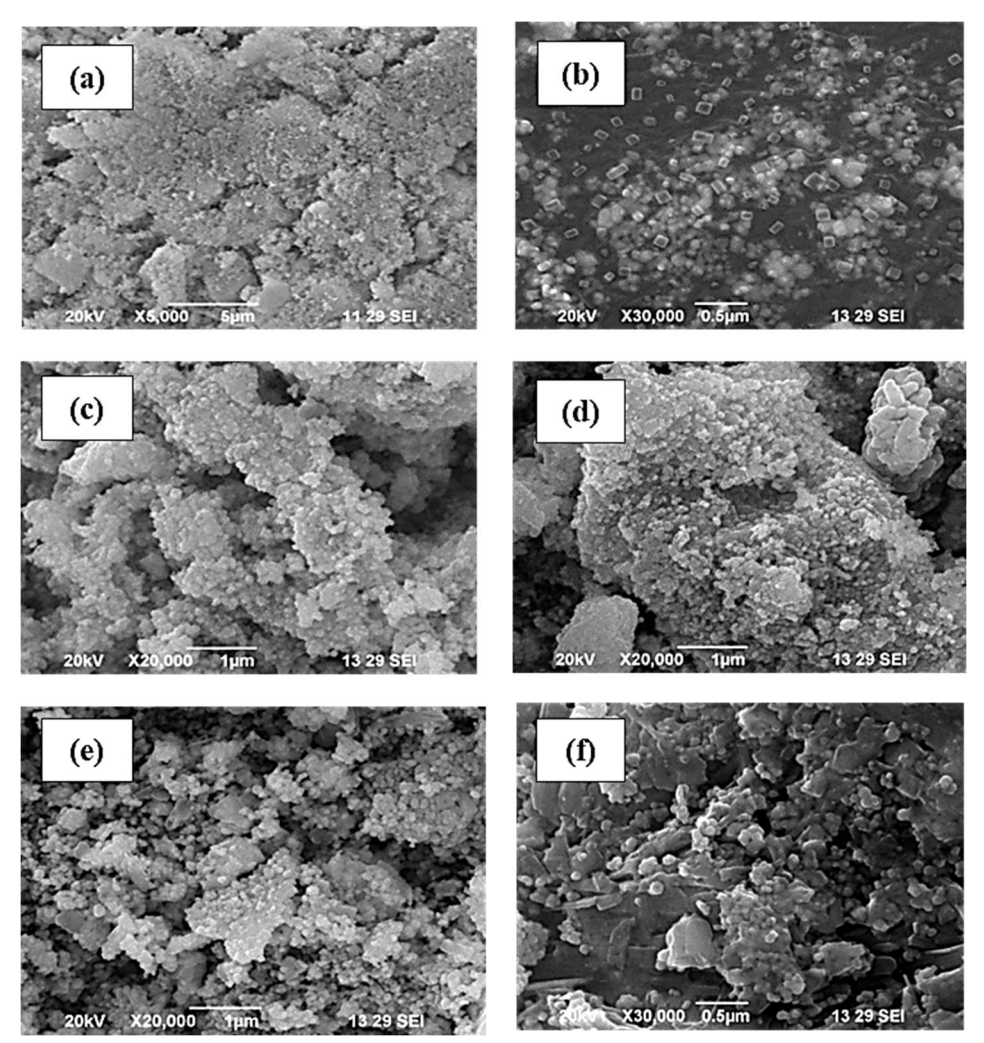


Figure 4. SEM photographs obtained on CeO_2 based nanoparticles a) Pure CeO_2 , b) $Ce_{0.90}Zn_{0.10}O_{2-\delta}$ c) $Ce_{0.80}Zn_{0.20}O_{2-\delta}$, d) $Ce_{0.70}Zn_{0.30}O_{2-\delta}$, e) $Ce_{0.60}Zn_{0.40}O_{2-\delta}$ and f) $Ce_{0.50}Zn_{0.50}O_{2-\delta}$

UV studies

To investigate the effect of Zn ion doping on the optical band-gap of the CeO₂ nanoparticles, UV-visible absorption study was carried out. The absorption spectra

for undoped and Zn doped CeO_2 nanoparticles were determined in the spectral range of 250nm -350nm as presented in Figure 5. A strong absorption peak is observed at 349nm by the incorporation of Zn ion at Ce

site. The peak shifted towards the lower wavelength side in the doped sample indicated a change in the electronic band structure. Using the absorption data, the energy gap (E_g) of the samples were estimated from Tauc equation [32-33] using the Equation (5)

where 'A' is proportionality constant, 'h' is the Planck's constant, 'v' is the frequency of vibration, 'hv' is the photon energy, 'α' is the absorption coefficient and 'n' is either 2 for direct band transitions or ½ for indirect

band transitions. The absorption coefficient (α) has been calculated using the relation (Equation 6)

$$\alpha = 2.303(A/t)$$
 (eq. 6)

where 't' is thickness and 'A' is optical absorbance. The energy band gap (E_g) is estimated by extrapolating the linear region of a plot of $(\alpha h \nu)^2 vs$ hv shown in the Figure 6. It was observed that the band gap of Zn doped CeO₂ nanoparticles is found to be in the range of 3.0 to 3.19 eV and our results are in close agreement with the reported data [33-34].

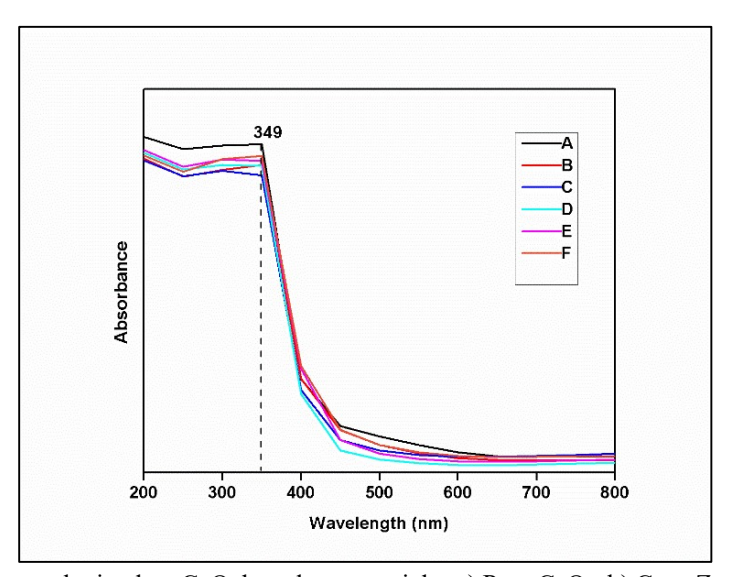


Figure 5. UV-visible spectra obtained on CeO_2 based nanoparticles a) Pure CeO_2 , b) $Ce_{0.90}Zn_{0.10}O_{2-\delta}$, c) $Ce_{0.80}Zn_{0.20}O_{2-\delta}$, d) $Ce_{0.70}Zn_{0.30}O_{2-\delta}$, e) $Ce_{0.60}Zn_{0.40}O_{2-\delta}$ and f) $Ce_{0.50}Zn_{0.50}O_{2\delta}$

Photoluminescence studies

The optical, electronic and photochemical properties of the materials can be well studied by photoluminescence (PL) studies [35-36]. PL spectra of Zn doped CeO₂ nanoparticles are reported in Figure 7. This spectra show two emission peaks, one at 395 nm to 425 nm which may correspond to band gap excitonic emission and another one located in between 500 nm to 520 nm which may relate to the presence of surface defects. The occurrence of strong and broad peaks reveals that the fabricated CeO₂ based nanoparticles are pure and crystalline [37]. Based on the above results, UV light source has been utilized for the photodegradation experiments. The best

photochemical properties are shown by $Ce_{0.60}Zn_{0.40}O_{2-\delta}$ nanophotocatalyst.

Photocatalytic studies

The photocatalytic activity Zn doped CeO_2 nanoparticles was performed for Rh B dye under UV light illumination. The photodegradation curves obtained the presence of CeO_2 based nanophotocatalysts with Rh B dye and Rh B dye alone without nanophotocatalysts are shown in Figure 8. The results revealed that the optimum photocatalytic efficiency (54.9 %) was shown by $Ce_{0.60}Zn_{0.40}O_{2-\delta}$ after 60 minutes of UV irradiation compared to the other compositions. Thus, the 40 mol% Zn doped CeO_2 nanophotocatalyst

was used as an optimized material to study the photocatalysis with respect to effect of pH and dye concentration. The photocatalytic degradation of the RhB dye can also be understood by plotting a first-order kinetic plot (Figure 9) described by Langmuir and Hinshelwood kinetic model [38]. The rate constant 'k' is calculated by using the Equation 7.

$$lnC_t/C_0 = -kt (eq. 7)$$

Where 'C₀' is the concentration at the beginning, 'C_t' is the final concentration and 'k' is the first order rate constant. The rate constant values were found to be 0.08 min⁻¹ (CeO₂), 0.005 min⁻¹ (Ce_{0.90}Zn_{0.10}O_{2- δ}), 0.007 min⁻¹ (Ce_{0.80}Zn_{0.20}O_{2- δ}), 0.012 min⁻¹ (Ce_{0.70}Zn_{0.30}O_{2- δ}), 0.016 min⁻¹ (Ce_{0.60}Zn_{0.40}O_{2- δ}) and 0.012 min⁻¹ (Ce_{0.50}Zn_{0.50}O_{2- δ}).

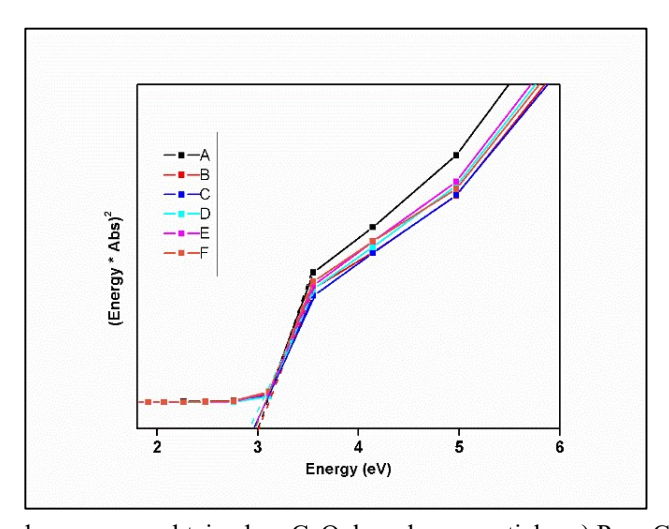


Figure 6. The band gap curves obtained on CeO₂ based nanoparticles a) Pure CeO₂, b) $Ce_{0.90}Zn_{0.10}O_{2-\delta}$, c) $Ce_{0.80}Zn_{0.20}O_{2-\delta}$, d) $Ce_{0.70}Zn_{0.30}O_{2-\delta}$, e) $Ce_{0.60}Zn_{0.40}O_{2-\delta}$ and f) $Ce_{0.50}Zn_{0.50}O_{2-\delta}$

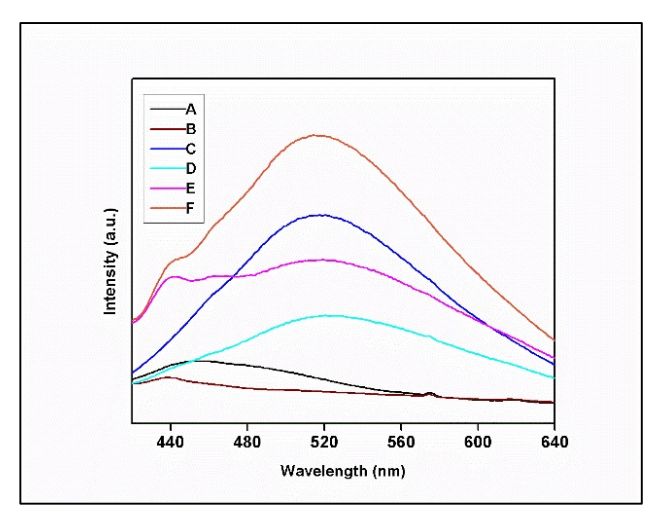


Figure 7. The PL spectra obtained on CeO_2 based nanoparticles a) Pure CeO_2 , b) $Ce_{0.90}Zn_{0.10}O_{2-\delta}$, c) $Ce_{0.80}Zn_{0.20}O_{2-\delta}$, d) $Ce_{0.70}Zn_{0.30}O_{2-\delta}$, e) $Ce_{0.60}Zn_{0.40}O_{2-\delta}$ and f) $Ce_{0.50}Zn_{0.50}O_{2-\delta}$

Influence of pH

The most important parameter to control the adsorption process is pH [39]. The pH of the dye solution in the present study was adjusted by the addition of dilute hydrochloric acid and dilute sodium hydroxide. To this study, pH values, such as, 2.5, 4.3, 6.5, 9.0 and 11.0 were fixed and the photodegradation efficiency was measured after irradiation in UV light source for one hour. The influence of pH value on the photocatalytic efficiency of Rh B dye in the presence of $Ce_{0.60}Zn_{0.40}O_{2-\delta}$ (best sample) is shown in Figure 10. The photocatalytic phenomenon is optimum (58.71%) at pH 9 in comparison with other pH values. Generally, the dye removal efficiency is minimal at low pH ranges [40].

Influence of concentration of dye

The photocatalytic efficiency of the best performing material (Ce_{0.60}Zn_{0.40}O_{2-δ}) was further studied at a standardized pH 9 of varying RhB dye concentrations, such as, 0.0025 g/L, 0.005 g/L, 0.0075 g/L and 0.01 g/L after 60 minutes under UV irradiation. Figure 11 shows the influence of RhB dye concentration on the photocatalytic efficiency of Ce_{0.60}Zn_{0.40}O_{2-δ} (best sample). The results revealed that the optimum photocatalytic efficiency is found at 58.71% for the dye concentration of 0.005g/L at pH 9. It was reported that the photodegradation is highly dependent on the probability of creation of OH radicals on the catalyst surface during the reaction process. If the concentration of dye is very high, it will retard the reaction between the dye molecules and OH radicals. Hence, optimum concentration of dye is required to have better efficiency of photodegradation process [41].

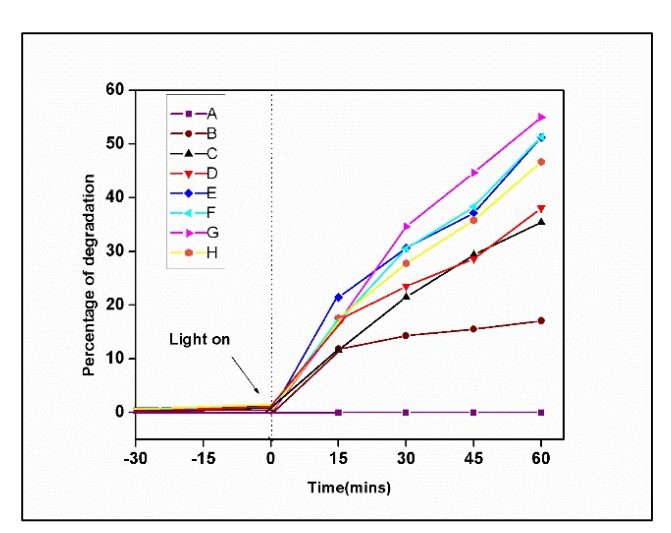


Figure 8. Photodegradation curves obtained in presence of CeO_2 based nanophotocatalysts with RhB dye and RhB dye alone without nanophotocatalysts a) RhB alone in dark, b) RhB alone in light, c) Pure CeO_2 , d) $Ce_{0.90}Zn_{0.10}O_{2-\delta}$, e) $Ce_{0.80}Zn_{0.20}O_{2-\delta}$, f) $Ce_{0.70}Zn_{0.30}O_{2-\delta}$, g) $Ce_{0.60}Zn_{0.40}O_{2-\delta}$, h) $Ce_{0.50}Zn_{0.50}O_{2-\delta}$

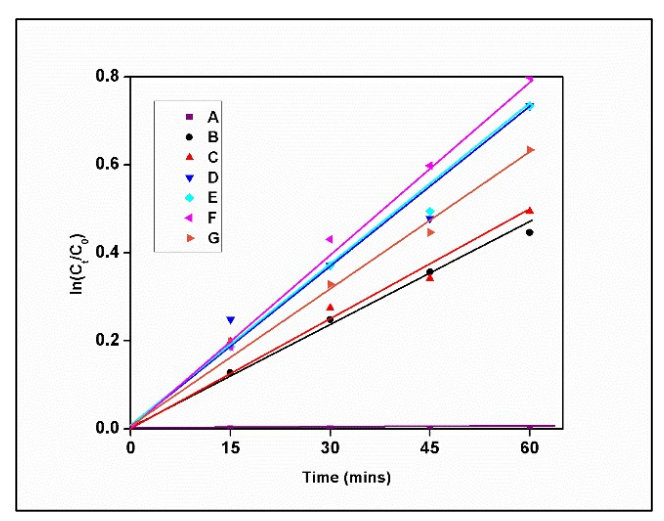


Figure 9. First order kinetic plot of RhB dye using a) RhB alone in the absence of photocatalyst, b) Pure CeO₂; c) $Ce_{0.90}Zn_{0.10}O_{2-\delta}, d) \ Ce_{0.80}Zn_{0.20}O_{2-\delta}, e) \ Ce_{0.70}Zn_{0.30}O_{2-\delta}, f) \ Ce_{0.60}Zn_{0.40}O_{2-\delta}; \ G) \ Ce_{0.50}Zn_{0.50}O_{2-\delta}$

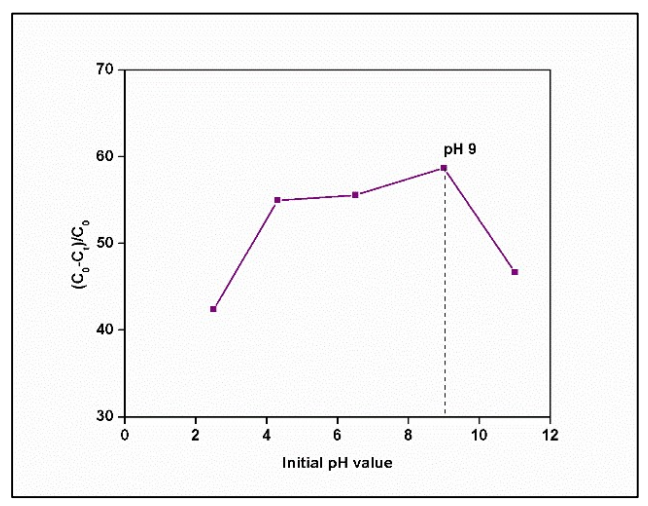


Figure 10. The influence of pH value on the degradation efficiency of RhB in presence of $Ce_{0.60}Zn_{0.40}O_{2-\delta}$ photocatalyst material

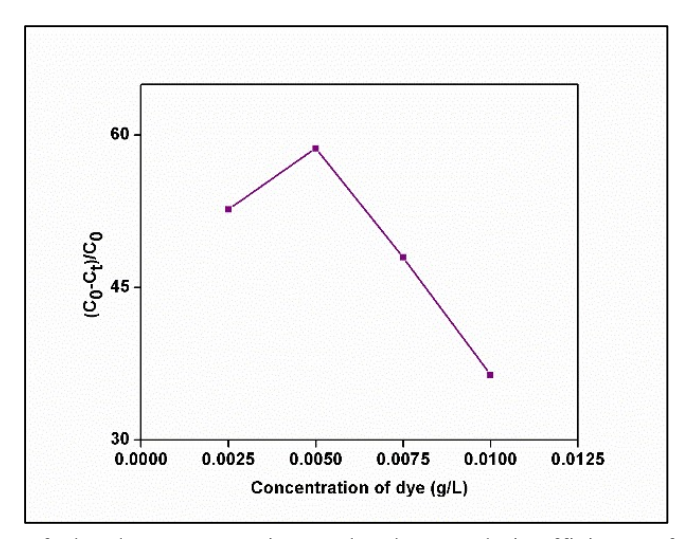


Figure 11. The influence of RhB dye concentration on the photocatalytic efficiency of Ce_{0.60}Zn_{0.40}O_{2-δ} nanoparticle

Conclusion

Simple wet chemical method was adopted for the preparation of pure CeO2 and Zn doped CeO2 (Ce1- $_{x}Zn_{x}O_{2-\delta}$; where x=0, 0.10, 0.20, 0.30, 0.40 and 0.50) nanoparticles in this research work. All the samples were assigned with cubic (F.C) crystalline structure based on XRD analysis. FTIR data confirmed the presence of M-O bond in the samples. EDX analysis reported the presence of Ce, Zn and O in the powder particles with appropriate concentration. Agglomeration of grains was revealed by SEM. The UV-visible spectra showed strong absorption peak around 349nm (λ_{max}) in all the composition of CeO₂ samples. The E_g of Ce₁. $_{x}Cu_{x}O_{2-\delta}$ was found to be in the range of 3.0eV - 3.19eV. The PL spectra of samples exhibited two peaks, viz., at 420nm (blue emission) and the other at 520 nm (blue emission). The photocatalysts, such as, CeO₂, $Ce_{0.90}Zn_{0.10}O_{2-\delta},$ $Ce_{0.80}Zn_{0.20}O_{2-\delta}$, $Ce_{0.70}Zn_{0.30}O_{2-\delta}$, $Ce_{0.60}Zn_{0.40}O_{2\text{-}\delta}$ and $Ce_{0.50}Zn_{0.50}O_{2-\delta}$ delivered a photocatalytic degradation efficiency of 35.46, 38.06, 51.25, 51.30, 54.97 and 46.69 % at pH 4.3 under illumination of UV light after 60 minutes. The parameters like, effect of pH and effect of initial concentration of dye were studied for the best sample $Ce_{0.60}Zn_{0.40}O_{2-\delta}$. At different pH values of 2.5, 4.3, 6.5, 9 and 11, the photocatalytic efficiency for Ce_{0.60}Zn_{0.40}O₂- δ was found to be 42.39, 54.97, 55.59, 58.71 and 46.69% respectively. Therefore, among different $Ce_{0.60}Zn_{0.40}O_{2\text{-}\delta}$ compositions studied, exhibited excellent performance towards elimination

Rhodamine B dye (Rh B) with 58.71% efficiency under UV irradiation. Further, the results revealed that the degradation efficiency was found to be maximum at pH = 9 and at a concentration of 0.005 g/L of RhB under a path route of pseudo-first order kinetic reaction.

Acknowledgements

The authors acknowledge Karunya Institute of Technology and Sciences for providing the research facilities.

References

- Wasim, M., Ashraf, M., Tayyaba, S. and Nazir, A. (2019). Simulation and Synthesis of ZnO nanorods on AAO nano porous template for use in a MEMS device. *Digest Journal* of *Nanomaterials* and *Biostructures*, 14: 559-567.
- Liu, H., Liu, J., Xie, X. and Li, X. (2020). Development of photo-magnetic drug delivery system by facile-designed dual stimuli-responsive modified biopolymeric chitosan capped nanovesicle to improve efficiency in the anesthetic effect and its biological investigations. *Journal* of *Photochemistry* and *Photobiology B: Biology*, 202: 111716.
- Andryukov, B. G., Besednova, N. N., Romashko, R. V., Zaporozhets, T. S. and Efimov, T. A. (2020). Label-free biosensors for laboratory-based diagnostics of infections: Current achievements and new trends. *Biosensors*, 10(2):11.

- Souza, J. M. T., de Araujo, A. R., de Carvalho, A. M. A., Amorim, A. d. G. N., Daboit, T. C., de Almeida, J. R. d. S., da Silva, D. A. and Eaton, P. (2020). Sustainably produced cashew gum-capped zinc oxide nanoparticles show antifungal activity against *Candida parapsilosis*. *Journal of Cleaner Production*, 247: 119085.
- Ilager, D., Shetti, N. P., Malladi, R. S., Shetty, N. S., Reddy, K. R. and Aminabhavi, T. M. (2020). Synthesis of Ca-doped ZnO nanoparticles and its application as highly efficient electrochemical sensor for the determination of anti-viral drug, Acyclovir. *Journal* of *Molecular Liquids*, 322:114552.
- Kulkarni, D. R., Malode, S. J., Prabhu, K. K., Ayachit, N. H., Kulkarni, R. M. and Shetti, N. P. (2020). Development of a novel nanosensor using ca-doped ZnO for antihistamine drug. *Materials Chemistry and Physics*, 246: 122791.
- Shanbhag, M. M., Shetti, N. P., Kulkarni, R. M. and Chandra, P. (2020). Nanostructured Ba/ZnO modified electrode as a sensor material for detection of organosulfur thiosalicylic acid. *Microchemical* Journal, 159: 105409.
- Gadisa, B. T., Appiah-Ntiamoah, R. and Kim, H. (2019). *In-situ* derived hierarchical ZnO/Zn-C nanofiber with high photocatalytic activity and recyclability under solar light. *Applied Surface Science*, 491: 350-359.
- He, J., Zhang, Y., Guo, Y., Rhodes, G., Yeom, J., Li, H. and Zhang, W. (2019). Photocatalytic degradation of cephalexin by ZnO nanowire under simulated sunlight: Kinetics, influencing factors, and mechanisms. *Environment International*, 132: 105105.
- Messih, M. A., Shalan, A. E., Sanad, M. F. and Ahmed, M. (2019). Facile approach to prepare ZnO@SiO₂ nanomaterials for photocatalytic degradation of some organic pollutant models. *Journal of Materials Science: Materials in Electronics*, 30: 14291-14299.
- 11. Vatchalan, L. and Pandiselvam, S. (2021). Carbon nano particles as better adsorbent against photocatalytic degrader for the rhodamine B dye.

- Journal of Water and Environmental Nanotechnology, 6(3): 232-240.
- 12. Deng, Y. and Zhao, R. (2015). Advanced oxidation processes (AOPs) in wastewater treatment. *Current Pollution Reports*, 1: 167-176.
- Francis, M. H., Sarkar, R., Roy, S., Jaffar, S., Mohan, V. R., Kang, G. and Balraj, V. (2016). Effectiveness of membrane filtration to improve drinking water: A quasi-experimental study from rural Southern India. *American Journal of Tropical Medicine* and *Hygiene*, 95(5): 1192-1200.
- El Nemr, A., Hassaan, M. A. and Madkour, F. F. (2018). Advanced oxidation process (AOP) for detoxification of acid red 17 dye solution and degradation mechanism. *Environmental Processes*, 5: 95-113.
- 15. Qi, K., Cheng, B., Yu, J. and Ho, W. (2017). Review on the improvement of the photocatalytic and antibacterial activities of ZnO. *Journal of Alloys and Compounds*, 727: 792-820.
- Liu, H., Li, L., Guo, C., Ning, J., Zhong, Y. and Hu, Y. (2020). Thickness-dependent carrier separation in Bi₂Fe₄O₉ nanoplates with enhanced photocatalytic water oxidation. *Chemical Engineering Journal*, 385:123929.
- Chong, M. N., Jin, B., Chow, C. W. K. and Saint, C. (2010). Recent developments in photocatalytic water treatment technology: A review. *Water Research*, 44 (10): 2997-3027.
- 18. Joshi, N.C., Gururani, P. and Gairola, S.P. (2022). Metal oxide nanoparticles and their nanocomposite-based materials as photocatalysts in the degradation of dyes. *Biointerface Research in Applied Chemistry*, 12(5): 6557-6579.
- Zhang, H., He, X., Zhang, Z., Zhang, P., Li, Y., Ma, Y., Kuang, Y. and Chai, Z. (2011). Nano-CeO₂ exhibits adverse effects at environmental relevant concentrations. *Environmental Science & Technology*, 45(8): 3725-3730.
- Majeed Khan, M. A., Khan, W., Ahamed, M. and Alhazaa, A. N. (2017). Microstructural properties and enhanced photocatalytic performance of Zn doped CeO₂ nanocrystals. *Scientific Reports*, 7: 12560.

- 21. Habib, I. Y., Muhammad, M., Yakasai, M. Y. and Abdullahi, A. D. (2021). Structural, morphological and optical properties of Ni-doped CeO₂ nanospheres prepared by surfactant free coprecipitation technique. *Open Journal of Science* and Technology, 4(4): 165-177.
- 22. Hou, X., Lu, Q. and Wang, X. (2017). Enhanced catalytic properties of La-doped CeO₂ nanopowders synthesized by hydrolyzing and oxidizing Ce₄₆La₅C₄₉ alloys. *Journal of Science: Advanced Materials and Devices*, 2(1): 41-44.
- Kumar, S., Al Omar, S. Y., Kumari, K., Albalwi, F., Kumar, R., Ahmed, F., Ahmed, N., Dwivedi, S. and Alvi, P.A. (2021). Electrical and antibacterial properties of Fe-doped CeO₂ nanoparticles. *Crystals*, 11: 1594.
- Nurhasanah, I., Sutanto, H. and Futikhaningtyas, R. (2014). Optical properties of Zn-doped CeO₂ nanoparticles as function of Zn content. *Advanced Materials Research*, 896: 108-111.
- Prabaharan, D. M. D. M., Sadaiyandi, K., Mahendran M. and Sagadevan, S. (2016). Structural, optical, morphological and dielectric properties of cerium oxide nanoparticles. *Materials Research*, 19(2): 478-482.
- 26. Wang, Z., Quan, Z. and Lin, J. (2007). Remarkable changes in the optical properties of CeO₂ nanocrystals induced by lanthanide ions doping. *Inorganic Chemistry*, 46(13): 5237-5242.
- 27. Jasmine Ketzial, J. and Samson Nesaraj, A. (2011). Synthesis of CeO₂ nanoparticles by chemical precipitation and the effect of a surfactant on the distribution of particle sizes. *Journal of Ceramic Processing Research*, 12(1): 74-79.
- 28. Thavarani, M., Charles Robert, M., Pavithra, N., Saravanan, R., Kannan, Y.B. and Balaji Prasath, S. (2022). Effect of Ca²⁺ doping on the electronic charge density and magnetic properties of ZnFe₂O₄ spinel ferrites. *Journal of Materials Science: Materials in Electronics*, 33: 4116-4131.
- Udayakumar, S., Renuga, V. and Kavitha, K. (2012). Synthesis and characterization of Ni doped ZnO by chemical precipitation method. *International Journal of Recent Scientific Research*, 3: 118-122.

- 30. Nandiyanto, A. B. D., Oktiani, R. and Ragadhita, R. (2019). How to read and interpret FTIR spectroscope of organic material. *Indonesian Journal of Science & Technology*, 4(1): 97-118.
- 31. Napitupulu, R. A. M. (2017). Influence of heating rate and temperature on austenite grain size during reheating steel. *IOP Conference Series: Materials Science and Engineering*, 237: 012038.
- 32. Arunkumar, M. and Samson Nesaraj, A. (2021). One pot chemical synthesis of ultrafine NiAl₂O₄ nanoparticles: Physico-chemical properties and photocatalytic degradation of organic dyes under visible light irradiation. *Inorganic and Nano-Metal Chemistry*, 51(6): 910-917.
- 33. Balogun, S.W., Sansui, Y. K. and Aina, A.O. (2018). Structural and optical properties of titanium dioxide thin film deposited by spin-coating technique. *International Journal of Development Research*, 8(1): 18486-18490.
- 34. Bhatia, S. and Verma, N. (2017). Photocatalytic activity of ZnO nanoparticles with optimization of defects. *Materials Research Bulletin*, 95: 468-476.
- 35. Amiri Gharaghani, M. and Malakootian, M. (2017). Photocatalytic degradation of the antibiotic ciprofloxacin by ZnO nanoparticles immobilized on a glass plate. *Desalination and Water Treatment*, 89: 304-314.
- 36. Chen, X. and Mao, S. S. (2007). Titanium dioxide nanomaterials: Synthesis, properties, modifications, and applications. *Chemical Reviews*, 107(7): 2891-959.
- 37. Sadiq, M. M. J. and Samson Nesaraj, A. (2013). Effect of surfactants in the synthesis of NiO nanoparticles by colloidal thermal assisted reflux condensation method. *Journal of New Technology Materials*, 3(2): 14-28.
- 38. Chandraboss, V. L., Natanapatham, L., Karthikeyan, B., Kamalakkannan. J., Prabha, S. and Senthilvelan, S. (2013). Effect of bismuth doping on the ZnO nanocomposite material and study of its photocatalytic activity under UV-light. *Materials Research Bulletin*, 48(10): 3707-3712.

- 39. Akpan, U. G. and Hameed, B. H. (2009). Parameters affecting the photocatalytic degradation of dyes using TiO₂-based photocatalysts: A review. *Journal of Hazardous Materials*, 170(2-3): 520-529.
- 40. Anju Chanu, L., Joychandra Singh, W., Jugeshwar Singh K. and Nomita Devi, K. (2019). Effect of operational parameters on the photocatalytic degradation of methylene blue dye solution using
- manganese doped ZnO nanoparticles. *Results in Physics*, 12: 1230-1237.
- 41. Jantawasu, P., Sreethawong, T. and Chavadej, S. (2009). Photocatalytic activity of nanocrystalline mesoporous-assembled TiO₂ photocatalyst for degradation of methyl orange mono azo dye in aqueous wastewater. *Chemical Engineering Journal*, 155 (1-2):223-233.